Scientific Program

Introduction

Solar2019

Introduction

Conference Proceedings

ASES National Solar Conference 2019

Minneapolis, Minnesota August 5-9, 2019

Introduction to SOLAR 2019 Proceedings

John Dunlop
Conference Chair
Principal, Renewable Energy Services LLC

The American Solar Energy Society believes that supplying 100% of America's electricity with renewable energy is not only possible but urgently necessary. We need to decarbonize our economy in order to have any chance of constraining the global temperature increase to less than 2 °C, which in itself will be disruptive to humankind.

ASES represents the scientists, educators, and activists who can provide renewable energy technologies and solutions for climate action in the United States that will have an immediate and large-scale impact. The ASES SOLAR 2019 Conference focused on those strategies.

The door for impacting climate change is rapidly closing. ASES intends to be a loud voice to follow the lead of states and cities across the country to decarbonize the nation's electricity supply and make an impact while that door is still open. We are in a race against time, and ASES believes we can win that race.

The ASES SOLAR 2019 Conference was held in one of the leading states for taking climate action, Minnesota. Minnesota has enacted climate policies that have provided leadership in the growth of wind power, solar power, community solar, variable generation integration technologies, energy efficient buildings and electrification of the transportation sector. But the strategies and solutions that were presented at the conference can – and must – be implemented across the country. Minnesota is pleased to host this important conference on taking climate action.

Many strategies will be necessary to take immediate climate action: electricity supply (residential, commercial, industrial, utility-scale solar; on land wind power; offshore wind power); transmission (including a national HVDC grid); electrifying the economy (transportation, homes, businesses, buildings); policies (international, national, state, intra-state, city); public support (social media; popular press, education); and personal actions (renewable energy opportunities; energy efficiency, electric vehicles).

Nearly 300 attendees from across the country converged at the Crowne Plaza Aire Hotel near the MSP Airport to share their concerns and solutions for addressing the climate crisis. Keynote speakers highlighted the need for urgent action. Global temperatures must rise no more than 0.5 deg C above today's temperatures in order to avert the worst impacts of climate change.

The conference focused on the role renewable energy can play in curbing climate change. The strong conclusion from the conference is that carbon emissions must be eliminated from the electricity and electrified transportation and new building sectors within just two decades. A rapid increase in electric power generated by renewables – primarily wind and solar power – will dramatically offset carbon emissions from burning fossil fuels and provide enormous investment opportunities.

doi:10.18086/solar.2019.00.01 Available at http://proceedings.ises.org

New large-scale wind and solar projects need to be built where the resources are strongest – the wind-rich Plains states and the solar-rich southwest states. In order to get the lowest-cost renewable electricity to the cities where it is needed, conferees were told, a new network of narrow, ultra-high voltage direct current (HVDC) power lines needs to be built to carry power across the country – not unlike the nation-wide Interstate highway system established back in the 1960's and 1970's, though HVDC power lines will not need to be strung through the center of population centers. A national HVDC network would make low cost renewable electricity available across the entire country.

But the conference also brought the message that solar resources are nearly as robust in both rural and urban communities anywhere in the country. New techniques are available to find appropriate sites for solar projects on homes and buildings in population centers, making renewable power available to the home/business and immediate community.

A major message from the conference is that people need to be bold in their commitment to taking climate action, and they must communicate the need for action among their colleagues, friends and families. They must also take personal climate actions, like switching to wind (through their utility) or solar power and be willing to talk about why they made the switch.

See www.ASES.org/conference for more information from the conference.

Solar2019

Conference Proceedings

ASES National Solar Conference 2019
Minneapolis, Minnesota August 5-9, 2019

ASES National Solar Conference 2019

PV Modeling as a Community Resource

John R. Bleem, Gerald P. Duggan, Wendell Stainsby, Daniel Zimmerle
Colorado State University, Fort Collins Colorado (USA)
bleemj@colostate.edu

Abstract

Northern Colorado communities have adopted policies that encourage utilities to implement 100% carbon free electricity by 2030. For example, Fort Collins is adding a new PV solar system nearly every day (350 in 2018) to support their climate and energy policy goals. Accurate PV modeling is well established, but often too complex to be readily employed in education or for use by municipal utility staff or energy researchers – the type of stakeholders needed to build community support for solar energy. Colorado State University has developed PV-STEM, a PV modeling tool that is both simple enough to teach solar engineering principals to STEM students and accurate enough to support local utility planning studies and university research. PV-STEM incorporates solar engineering principles developed by NREL, Sandia National Labs and NOAA into an open-source Python code accessible to novice software programmers that only requires commonly available PV system and local weather information. The model has been validated against ten operating PV systems and against PVWatts®. In addition to STEM education, the model has been used to enhance understanding of PV generation on the community's electric distribution system (generation profiles, PV customer load research, policy analysis, resource forecasting, etc.). User guidelines, teaching slides and open source Python code will be available for interested parties.

Keywords: *PV modeling, STEM education, community resource planning*

1. Introduction

Colorado State University (CSU) is a major employer and a highly engaged member of the Fort Collins, Colorado community (City). Both CSU and the City have climate action plans with goals of carbon neutrality by 2050, including 100% renewable electricity use by 2030. These goals are being met in collaboration with the local electricity supplier (Platte River Power Authority), combining wholesale and distributed renewable resource additions. As of August 2019, about 1,600 residential photovoltaic (PV) solar systems have been installed on the City's distribution grid, encouraged by rebates, feed-in tariffs and net metering incentives (see Figure 1). A few large commercial systems were installed during 2015 (in response to the feed-in tariff program), but the vast majority of systems are installed on residential sites within the community. Though the City collects advanced metering infrastructure (AMI) data for all residential customers, very little PV system generation data is available for residential systems. AMI meters only provide net metered data regarding power flow (amounts delivered from the utility and amounts received by the utility from solar customers). By combining estimated generation from PV-STEM modeling with AMI data, estimated load profiles can be developed for residential solar customers (i.e. for the "solar" rate class in the City). Other projects that require estimated PV production, such as studies of high PV penetration in distribution systems, can also benefit from application of PV-STEM.

doi:10.18086/solar.2019.01.02 Available at http://proceedings.ises.org

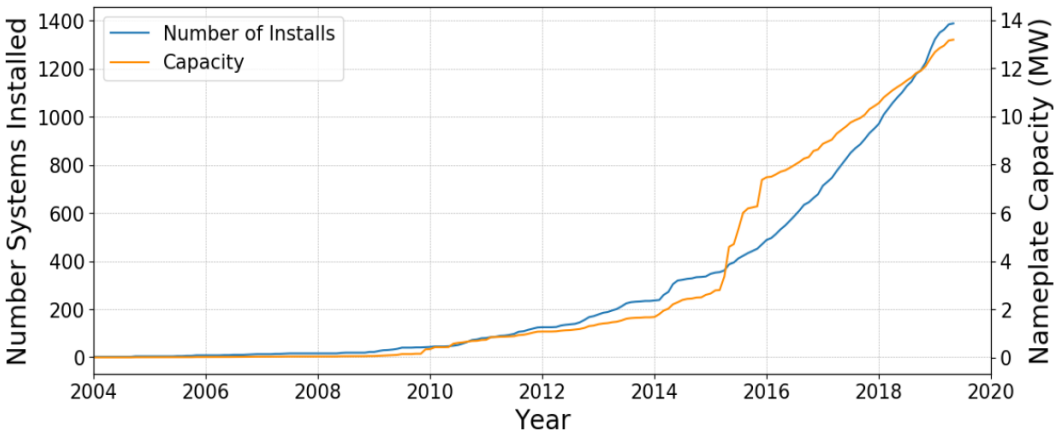

Figure 1: Growth of distributed PV solar systems in the City

A significant number of PV modeling programs exist, including PVWatts®, developed by the National Renewable Energy Laboratory (NREL). However, existing models have characteristics that make them unattractive for community-based PV modeling. These models typically: a) are proprietary, requiring a commercial license (with associated cost); b) use typical meteorological year (TMY) weather data, a long-term average rather than actual historical values; c) are limited to hourly time intervals (or longer); d) run one system at a time; and/or e) require detailed input data that is not available to community or educational users. These models are also somewhat limited in terms of use as an educational tool, since the source code is proprietary or complex, and difficult to change for either educational or project needs.

2. Modeling Methodology

The PV-STEM model is targeted at 'community' niche applications. It is neither too technical (hard to implement) nor too simple (able to maintain good accuracy), contains no proprietary software, is accessible to novice programmers, is flexible (allowing coding changes for unique projects), and requires modest data inputs that are likely to be available to community users. The tool is designed for STEM (science, technology, engineering, mathematics) teaching, as well as research and electric utility planning.

PV-STEM utilizes PV modeling algorithms available from the NREL, Sandia National Laboratories (SNL) and the National Oceanic and Atmospheric Administration (NOAA). Weather data from many sources can be used. For examples provided here, we use data from the National Climate Data Center and CSU"s main campus weather station. Other weather stations and monitoring data from other locations within the community may also be used for modeling. An overview of the modeling approach is provided in Figure 2.

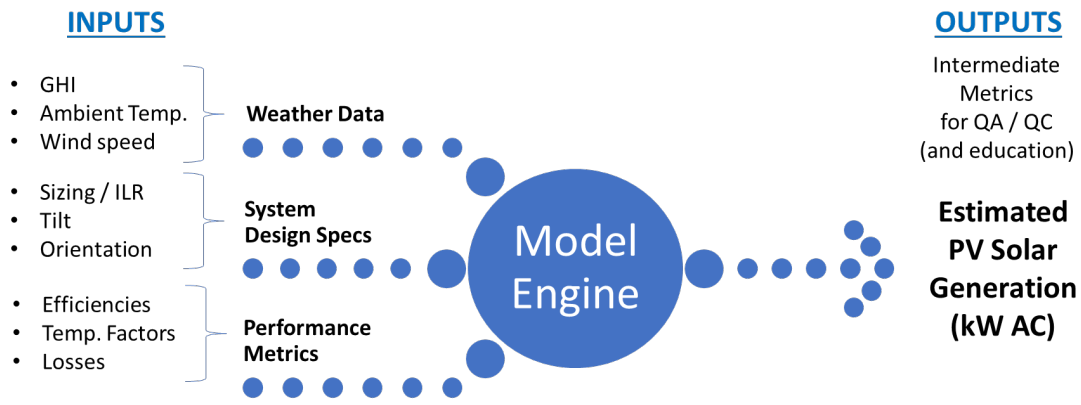

Figure 2: Overview of PV-STEM model

Key steps involved with the PV-STEM modeling process include:

- Establish time conventions and alignments
- Determine extraterrestrial irradiance – direct normal and horizontal – to support Erbs method
- Split measured irradiance (global horizontal) into beam and diffuse components
  - Erbs piecewise curve fitting used (see documentation)
- Adjust beam to plane of array magnitude:
  - Tilt, azimuth & ground reflectance
- Calculate total plane of array irradiance (beam plus diffuse plus ground reflected) – W/m^2
- Use system-specific metrics to calculate generation (kW):
  - DC & AC ratings and other design metrics
  - Efficiencies → modules, inverter, system
  - Temperature degradation metrics / algorithms
  - Losses → wiring, outages, snow, shading, soiling, etc.

Full details of the modeling approach are described in PV-STEM documentation, slides / training materials and source code. These materials will be available from the CSU Energy Institute (Powerhouse Campus), anticipating distribution by September 2019. See https://energy.colostate.edu/about/the-powerhouse/ for information.

3. Model Validation

PV-STEM has been verified through two approaches: (1) comparison with actual hourly generation from existing systems, and (2) comparison with PVWatts®. Though very few residential systems in the City have metered generation data available, this data has been gathered from commercial systems operating in the community. Ten existing systems were used to compare actual historical generation (provided by the solar unit's data acquisition system or DAS) with estimated generation from the PV-STEM model. For comparison with PVWatts®, several sets of tilt and orientation combinations were run with both models for a "generic" 100 kW PV solar system.

As an interim validation step for model verification, sun position values determined from PV-STEM were compared with values provided from two well established tools: (1) NOAA's Solar Calculator, and (2) NREL's Solar Position Algorithm. Results compare very favorably, with PV-STEM and existing models differing by only small fractions of a degree for each of the critical angles tested (zenith/altitude, azimuth and angle of incidence). Links to on-line versions of these tools are included below:

https://www.esrl.noaa.gov/gmd/grad/solcalc/ (NOAA) and https://midcdmz.nrel.gov/solpos/spa.html (NREL)

Existing PV systems used for verification (those having historical generation data available) range in size from 20 kW to 632 kW. System azimuth values range from 140° to 185° with system tilt values of 1.5° to 30°. All systems are located within a radius of approximately two miles from the weather site collecting historical global horizontal irradiance (GHI), ambient temperature and wind speed data (CSU's Main Campus Weather Station). Values for actual historical generation are provided by the data acquisition system (DAS) equipment associated with each PV solar system. System specifications (size, age, equipment performance metrics, etc.) were gathered from system owners and/or operators. Losses associated with system age were estimated assuming 0.6% loss per year (0.05% per month), from the initial commercial operating date to the mid-point of the analysis period, based on typical specifications from manufacturers of the systems modeled. Modeling data was available for all test systems in the time range of 2016 to 2018, with 12 months of consecutive hourly data used to validate each system. Acquired data sets were cleaned to remove missing or faulty generation data. As a result, not every system was run for the same 12-month period.

Annual comparisons between PV-STEM and actual generation are shown in Figure 3, and monthly comparisons in Figure 4 for all ten systems (sizes of the systems considered are also shown in Figure 3). Values for "Difference" in these figures are calculated as the PV-STEM estimated value less the actual value, divided by the actual value. Note that the largest deviations between actual and modeled generation occur during months when snow accumulates on the panels and generation is lowest (i.e. winter months). PV-STEM includes approaches to estimate snow losses (see documentation). Also, during winter months, weather is cloudier, and errors associated with the Erbs curve fit application for estimating direct vs. diffuse irradiance has more influence on results (see

documentation for Erbs method). The model is most accurate during summer periods, when generation levels are highest. Overall, annual differences are small for the systems modeled (less than 5% on an annual energy basis).

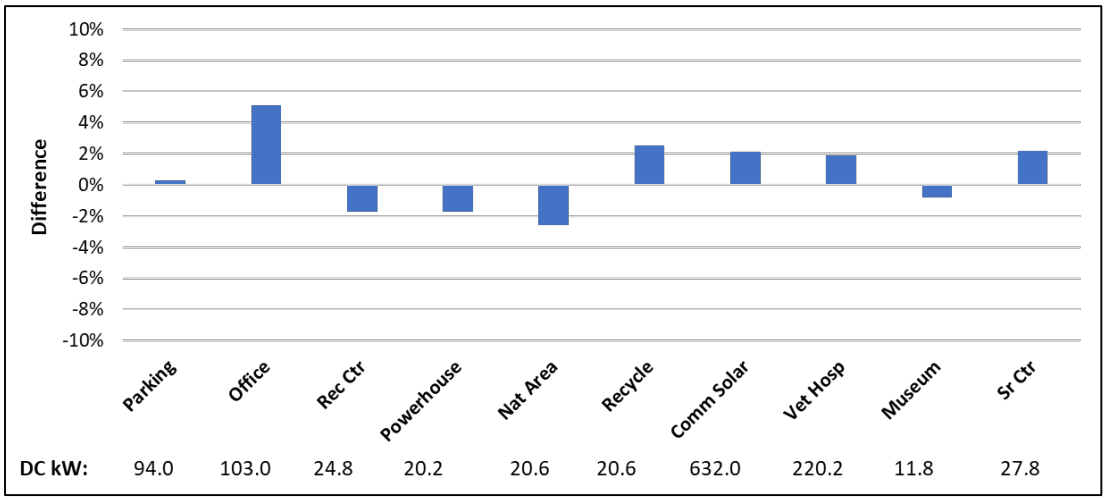

Figure 3: Annual generation differences

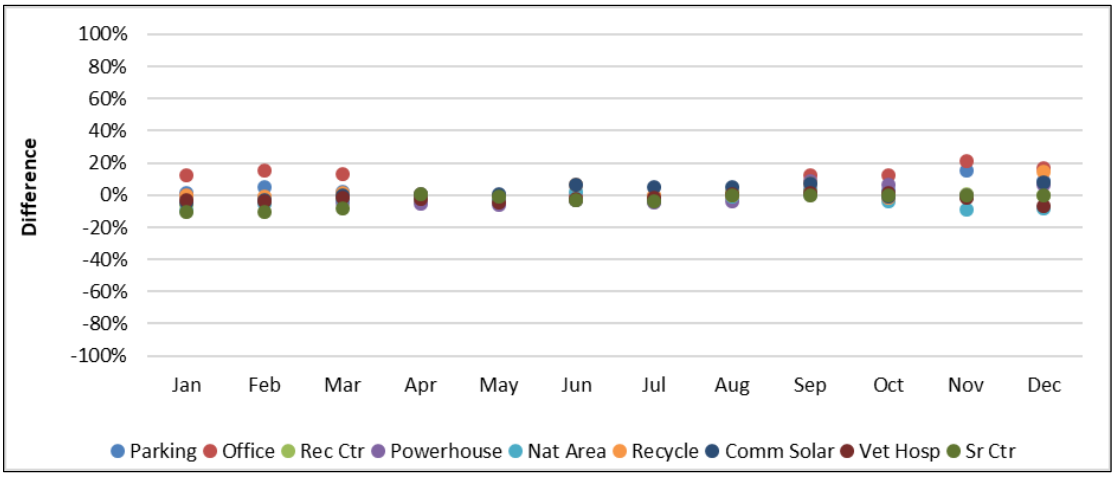

Figure 4: Monthly generation differences

Daily differences between the model and actual generation were also considered for verification. An example of this comparison is provided in Figure 5 (20.6 kW Nat Area site).

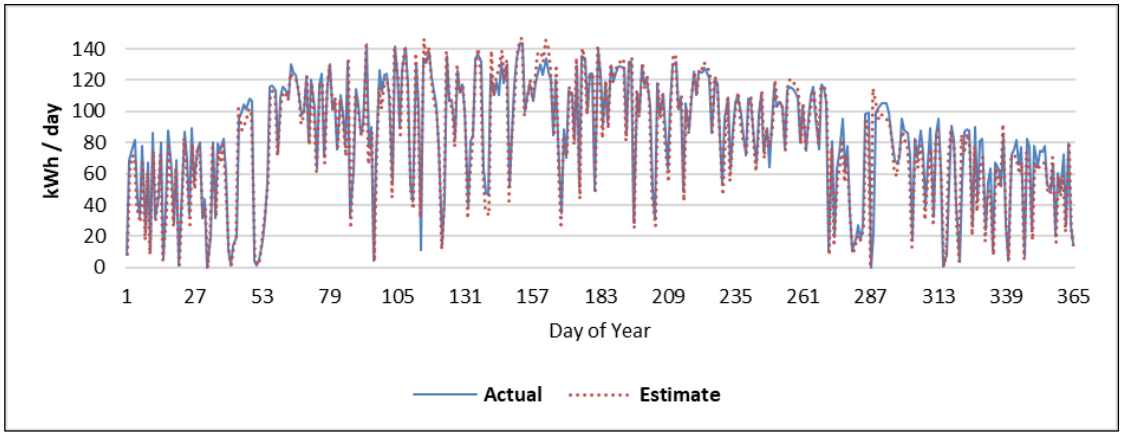

Figure 5: Example of daily generation comparison

Note that in this case, not all of the snow losses are captured by the model (snow clearing took longer than the model estimated). This is true for most of the comparisons. PV-STEM can be applied using two approaches for snow: (1) when comparing actual generation values with model estimates, and (2) when the model is used to directly estimated generation (no actual values available). For the first case, it is assumed that snow clears from the GHI sensor immediately and the model value is taken as the "no snow" value. Clearing of snow from the system is based on snow event data (snowfall and accumulation). Often, this approach shows that snow is not cleared from the systems even when snowfall data indicates no snow accumulation for the weather data site.

In the second case (when no actual generation data available), estimates of snow losses are addressed through additional model algorithms – based on tilt and other factors (see model documentation). Estimating snow is a challenge, particularly for shorter term time periods, and model errors associated with snow clearing can be significant for hourly / daily time increments.

Annual, monthly and daily values are summed from hourly values (actual and PV-STEM estimates). An example of the hourly comparison for the Natural Areas site (20.6 kW) is shown in Figure 6 (example week in May 2018).

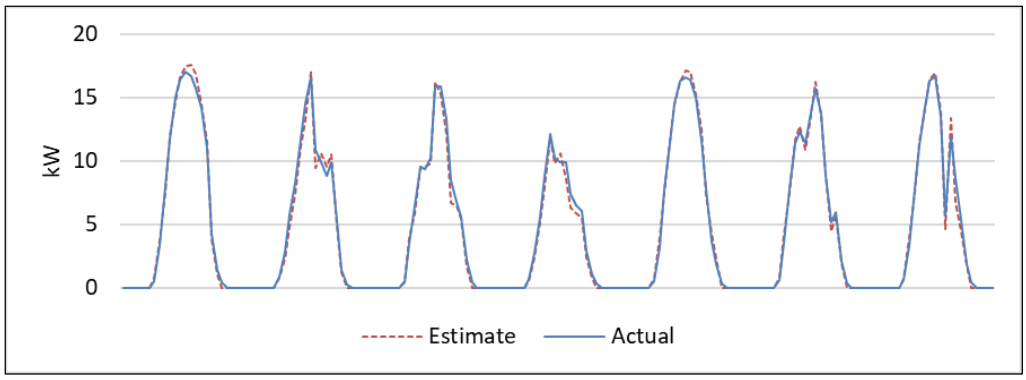

Figure 6: Example of hourly generation comparison

Hourly values (actual and modeled) were summed and compared for each system to further test validation of the PV-STEM model. Figure 7 shows an example of this summation.

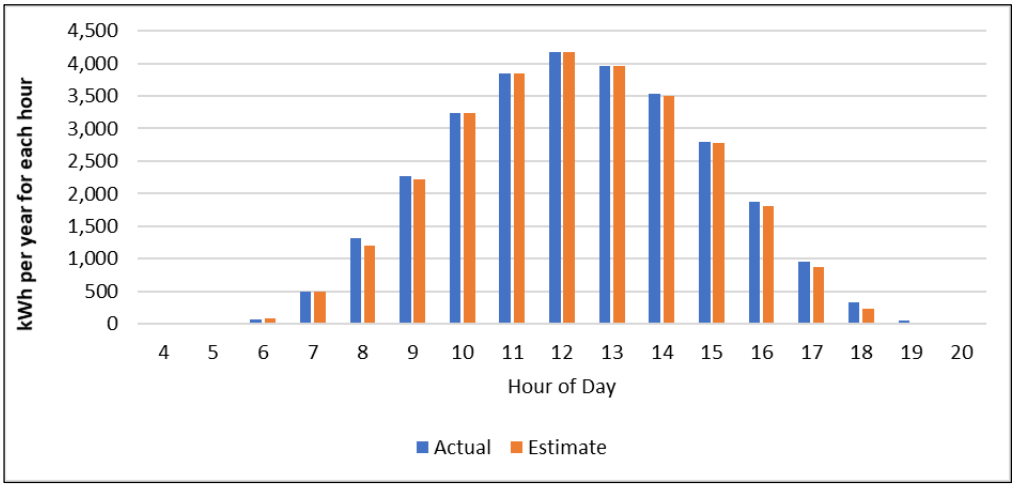

Figure 7: Example of hour-by-hour annual sum

Annual plots were also developed to track actual generation (measured by the specific PV system DAS) vs. estimated generation (from the PV-STEM model) for each hour of the entire year at each site modeled. An example is shown in Figure 8.

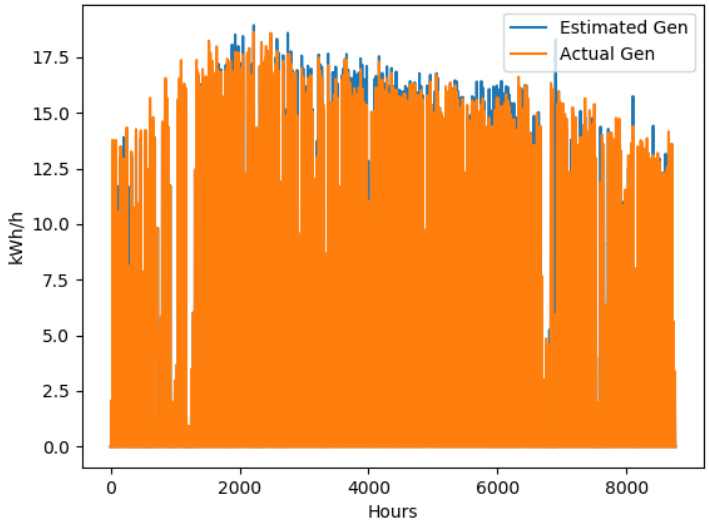

Figure 8: Example of full year hourly comparison for actual generation vs. PVSTEM estimated generation

As mentioned earlier, results from the PV-STEM model and PVWatts® runs were also compared. Fort Collins requires a PVWatts® run for estimating energy production from solar systems that are interconnected with the City's distribution system, so comparing these models was of interest to the PV-STEM team (and to the City). TMY weather data associated with the current version of PVWatts® were used as inputs to PV-STEM (global horizontal irradiance, ambient temperature and wind speed). The models were compared for a generic 100 kW system, having typical system parameters (defaults in the PVWatts® tool). Losses were handled identically in the two models, with losses for snow, aging and availability set to zero in both models. PVWatts® uses global horizontal irradiance (GHI), direct normal irradiance (DNI) and diffuse horizontal irradiance (DHI) values directly from the TMY data set to calculate total plane of array irradiance. PV-STEM estimates the split of GHI into DNI and DHI based on the Erbs piecewise curve fit approach (see details and references in model documentation).

Several sets of tilt / orientation values were analyzed using both models for the generic 100 kW system, with results provided below (annual comparison in Figure 9 and monthly in Figure 10). Results compare favorably and differences between PV-STEM and PVWatts® for these modeling sets were lower than those for the comparisons between actual generation and generation estimated by PV-STEM. These differences are attributed to handling of the following: GHI, DNI and DHI (as mentioned above), temperature-related losses, part-load inverter losses, and other differences between the models.

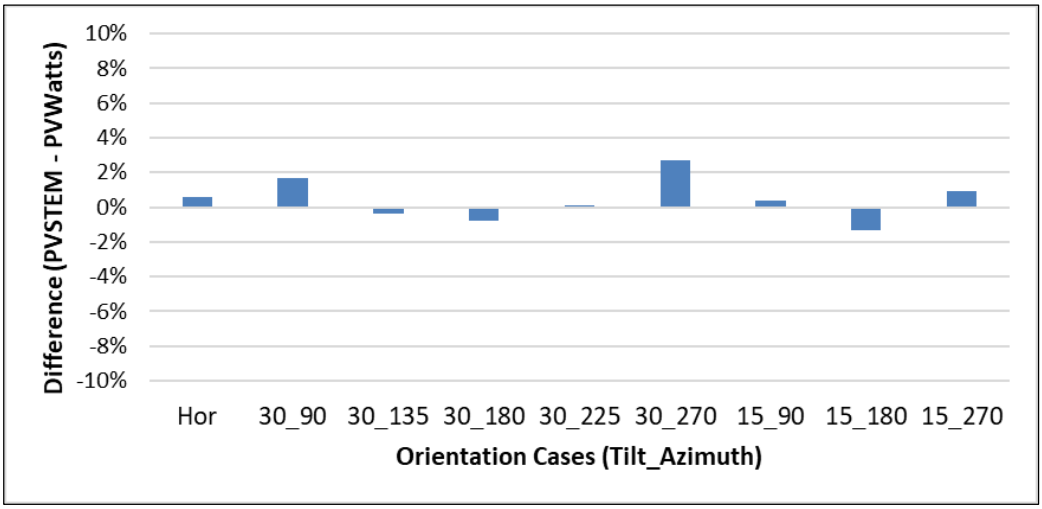

Figure 9: Annual PV-STEM vs. PVWatts® model comparisons

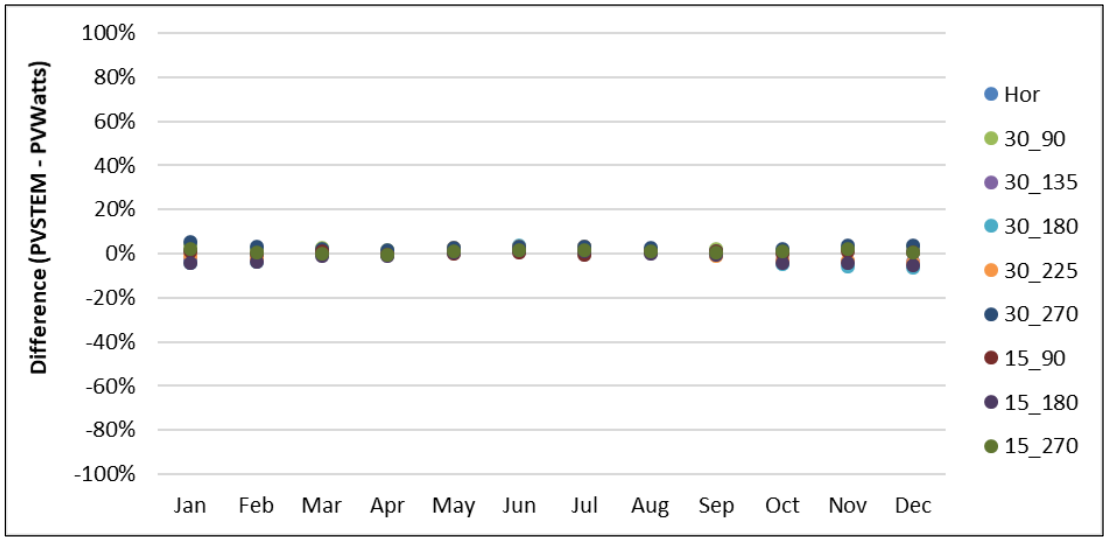

Figure 10: PV-STEM vs. PVWatts model comparisons (daily values)

PV solar systems in the community are typically mounted in parallel alignment with the roof, following standard practice for this region. Residential roof pitches in the City are typically in the range of 3/12 to 7/12 (14.0° to 30.3° tilt), so the PV-STEM model was run for cases in this range (to compare with PVWatts®).

As in the case of comparing actual generation with PV-STEM estimates, daily and hourly results were also compared for the PV-STEM vs. PVWatts® runs. Figure 11 provides example daily comparisons for the 30° tilt, 180° azimuth (30_180) case and Figure 12 shows an example of a full year hourly comparison. For this case, generation is highest in the spring and fall months. Systems with low tilt generate at their highest levels during summer periods (both models).

Note that a north facing case was also modeled, even though this is not ideal for this location (in the northern hemisphere). Differences in results for this case are similar, though daily and monthly errors are higher in the winter season for the north facing modeled case.

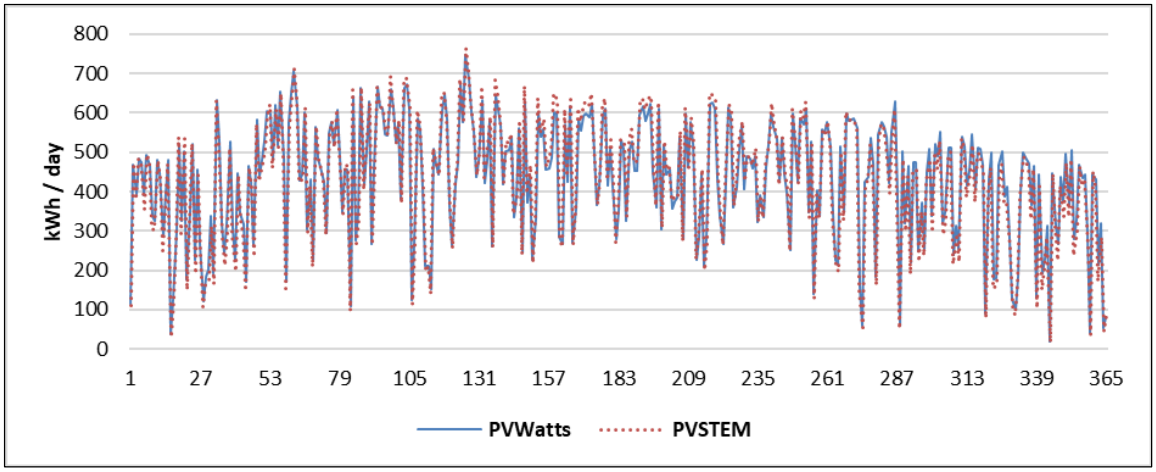

Figure 11: Example of Daily comparison for PV-STEM vs. PVWatts on 30° tilt, 180° azimuth (30_180 case)

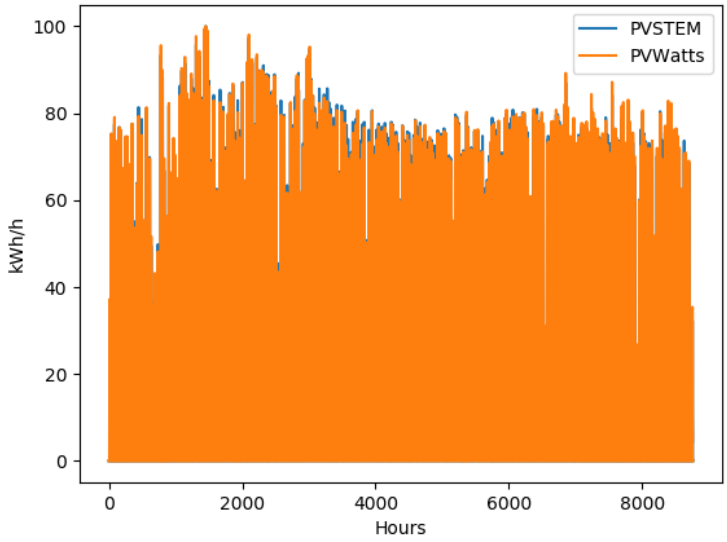

Figure 12: Example of full year hourly comparison for PV-STEM vs. PVWatts (30_180 case)

4. Model Applications

PV-STEM has been used to support several educational and planning activities in the community. A summary of applications to date is provided below:

- **Elementary school education** – the model supports solar design activities within STEM club and problem-based learning activities. Students are provided basic solar principles (through a lecture format), Then they design a system and install "panels" on small model buildings (non-operating replicas). PV-STEM is run for each of the systems and the system with the most production "wins" the design competition. Students are allowed to re-design and re-run the model with improved designs.
- **High school education** – high school students have been trained in Python coding and solar energy principles as part of extracurricular STEM activities. Students learn how to run the PV-STEM code in various configurations to gain experience in application of solar energy. The educational experience is enhanced through use of Google Earth® and Google Sunroof® online tools (also used by elementary students).
- **University education** – PV-STEM supported a thesis project at Colorado State University during 2019 and is available to support future graduate student work. It also is being integrated into solar-related research activities at the CSU Energy Institute and is reviewed as part of a graduate level mechanical engineering course at CSU.
- **Electric Utility research** – Fort Collins is a non-profit municipal utility, owned by the members of the community. Many collaborative projects have been conducted between CSU and the City. One recent project utilizing PV-STEM involves enhancing the understanding of residential PV solar generation characteristics in the City. Net electric load/generation (AMI) data is available in 15-minute increments for residential systems (from utility smart meters). A database of residential PV system characteristics is also being updated, which can provide input metrics for system modeling (size, tilt, azimuth, etc.). PV-STEM is being applied to provide estimates of generation patterns for individual customer installations at a granular level (15-minute metering increments). PV system output from the model can be combined with measured net load/generation data to estimate premise electricity use (shown graphically in Figure 13). Generation and usage estimates can also be aggregated to provide insights regarding PV generation operations across the City utility distribution network, supporting future planning efforts (rate design, limits on solar sizing, PV resource expansion, etc.).

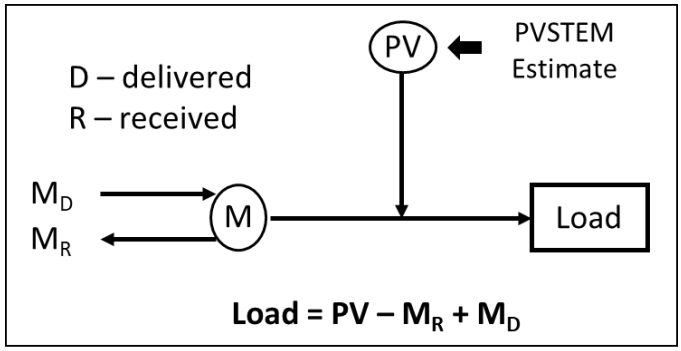

Figure 13: Schematic of approach for estimating solar customer load profiles

- **"She's In Power" program** – She's in Power is an initiative of Colorado Clean Energy Education and Empowerment (C3E), designed to grow and inspire the women who will be tomorrow's clean energy leaders and reduce greenhouse gases in the City, innovating a more sustainable community today and developing the diverse clean energy workforce of tomorrow. As a "Spark" in this program, students work with a project team to learn solar engineering principals and apply them through use of the PV-STEM model and other tools. This program provides student and Energy Institute staff to support the electric utility research mentioned above. Other projects and general information regarding the program can be viewed at this link: https://coloradoc3e.org/shes-in-power/.
- **Community-wide solar modeling** – PV-STEM is also being developed as a tool to provide estimates of total solar energy production occurring within the City (from distribution level PV systems), and to share this information with the community on a near real-time basis (e.g. every hour). Additional monitors, web site development / graphics and communications will be required to complete this effort.

Additional applications for PV-STEM will be identified as distributed solar energy continues to expand in the City and the region. Enhancements to the model are anticipated as it is applied to support future PV solar projects. Shading is a primary concern, which can be incorporated into the model using existing solar position algorithms and adding loss factors for solar positions related to shading obstacles at a given site. Additional work can also be done to improve the snow loss algorithms in the model. We hope to engage more students and educators in the ongoing process for improving the model over time (and finding new applications) – in order to continue supporting solar education, research and communications in our community.

Conference Proceedings

ASES National Solar Conference 2019

Minneapolis, Minnesota August 5-9, 2019

A Study on the Thermal Energy Storage System Using Multiple PCMs

Omer S. Elsanusi[1], Emmanuel C. Nsofor[1]

[1] Department of Mechanical Engineering and Energy Processes, Southern Illinois University Carbondale, Carbondale, IL, (USA)

oelsanusi@siu.edu

Abstract

Application of Phase Change Materials (PCMs) for energy storage has been found to exhibit high potential due to the high energy storing capacity. This study investigated the performance of multiple PCMs in a number of energy storage systems. The effects of conduction and natural convection on these systems were also studied. Numerical simulations based on the conservation equations were conducted on the defined geometries. It was found that natural convection has significant positive effects on the heat transfer in these systems. It was also found that application of multiple PCMs generally enhances performance. However, different effects were observed on the heat transfer mechanisms. The parallel configuration enhances conduction but suppresses convection while the series configuration does the opposite. It was also found that the vertical orientation enhances convection more than the horizontal orientation for the multiple PCMs configurations. Energy storage with the series configuration in vertical orientation was found to be superior with 47% and 60% reduction in complete melting time respectively, compared to the single configuration in vertical orientation and to the single and series configurations (horizontal and vertical) in the conduction only case.

Keywords: *Phase Change Materials, Renewable Energy, Heat Transfer*

1. Introduction

Renewable energy sources such as solar, wind and hydro have the potential to address the energy challenges facing the world. The challenges include continued increase in energy consumption and demand due to population growth and the changing ways of life. This demand increase is faced with expectations of fossil fuels depletion and the environmental hazards associated with their extraction, transportation and consumption. One major obstacle that all renewable energy sources have to overcome is their inherited fluctuations in nature. This is why it is crucial to develop efficient means of energy storage.

Considering solar energy, thermal energy storage (TES) presents high potential and could be a very reasonable means for addressing the fluctuation issue. TES systems are classified into three methods namely sensible heat, latent heat and thermochemical storage methods [1]. Latent heat storage method has the advantage of the high energy storing density available in Phase Change Materials (PCMs). However, there are challenges

doi:10.18086/solar.2019.01.03 Available at http://proceedings.ises.org

that need to be addressed in order to efficiently apply its use on commercial scales. PCMs suffer when it comes to thermal conductivity. Their low thermal conductivity leads to low heat transfer rates and hence to slow energy storage and recovery processes.

One way to overcome this limitation, is by developing new phase change composites with the aid of additives. Potential additives that have been studied include porous graphite and metallic matrices, dispersing metal particles, carbon fibers and nanotube amongst others. Poly vinyl Pyrrolidone (PVP) was used as a dispersing additive to enhance multi walled carbon nanotube MWCNT, graphite and graphene dispersion in liquid Steric Acid (SA). It was found that PVP provides good dispersion of additives in SA. It was stated [2] that as the percentage of additives was increased to 5%, they have a strong influence on the melting point, freezing point and latent heat of SA and reduced heat storage capacity due to reducing steric acid mass in these cases. Nano magnetite (Fe3O4) particles were added at different ratios to enhance the common PCM paraffin. 10% increment in heat storage capacity of Paraffin with melting point range of 46 to 48ºC was reported with the conclusion that further investigation and analysis are needed to determine the thermal stability and thermal conductivity of these composites [3]. According to Zabalegui et al. [4], there is a disadvantage of using nanoparticles to enhance PCMs' thermal conductivity as it was reported that reduction of latent heat of fusion occurred in response to the dispersion of MWCNT in paraffin. It was stated that Brownian motion, particle clustering and interfacial liquid layering are possibly the causes for this reduction. This points out that adding nanoparticles in PCMs may not provide significant enhancement in TES performance since thermal conductivity enhancement is faced with reduction in latent heat of fusion.

Other methods including the use of multiple PCMs are being investigated to enhance the heat transfer and hence the performance of these systems. The use of cascaded PCM of D-Mannitol and Hydroquinone has been evaluated. These PCMs have melting temperatures in the range of 150 – 200ºC. It was found that this configuration produces significant enhancement of about 19.4 % compared to the single PCM configuration. Moreover, the temperature difference in the heat transfer fluid between inlet and outlet was more uniform [5]. The effects of the number of PCMs used, the melting temperature difference between them and their mass ratios on the performance were investigated. It was reported that multi PCM configuration enhances TES performance more as the number of stages increases. However, this enhancement wasn't significant with applying more than three stages [6]. On the other hand, larger melting temperature difference between PCMs was found to enhance the performance significantly. Wang et al. [7] found that m-PCMs with unequal mass ratios produce better enhancement.

2. Materials and Methods

The method used in this study for investigating the performance of multiple families of PCMs in different configurations and orientations was inspired by the fact that heat transfer is directly proportional to temperature difference.

2.1 Geometry and Properties

Fig. 1 illustrates the PCM container with a working fluid circulating in the immersed piping. Multiple-PCMs under the arrangements were studied to understand the heat transfer and melting processes in the setup and

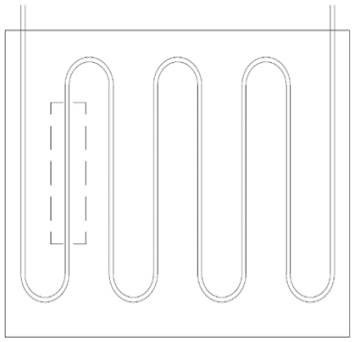

Fig. 1: PCM container with circulating working fluid

investigate the system performance. A small segment of the piping is considered as shown by the dashed line. This segment is modeled as a concentric pipe. The inner pipe that carries the working fluid has an inside radius (ri) of 7 mm and an outside radius (rt) of 8 mm. The outer radius surrounding the PCMs (ro) is 35 mm. This section of the pipe is 500 mm long. These dimensions are chosen to enable model validation with the study by Fornarelli et al. [8]. Under the assumption of axisymmetric conditions (except for the third case as will be discussed), a 2D model is considered. Three PCMs were considered with melting temperatures that range from 430 to 520 K, thermal conductivities from 0.4 to 0.5 W/m K, specific heats from 1400 to 1650 J/kg K and densities from 1500 to 2000 Kg/m3.

Three configurations of PCM were studied namely: (a) Single PCM configuration, (b) M-PCMs in series configuration and (c) M-PCMs in parallel configuration. These configurations describe how single or m-PCMs occupy the PCM container as shown in figure 2. The PCMs were arranged in the order of their melting points from high to low.

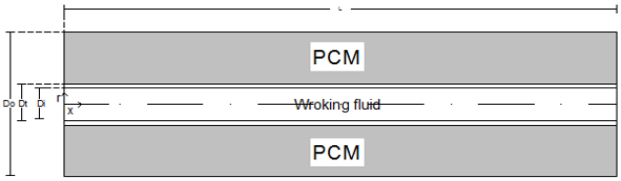

Fig. 2: Geometry under investigation

2.2 Mathematical Model

Heat transfer and fluid dynamics of this setup are characterized by velocity, temperature and liquid fraction of the working fluid and phase change materials. They are governed by the mass conservation equation, the momentum conservation equations and the energy equation. The energy equation is considered in the enthalpy form to account for the latent heat of melting as follows:

$$H = h + \Delta H \qquad \text{(eq. 1)}$$

$$h = h_{ref} + \int_{T_{ref}}^{T} c_p \, dT \qquad \text{(eq. 2)}$$

where H is Total enthalpy, h is sensible enthalpy and ΔH is latent enthalpy evaluated as:

$$\Delta H = \gamma L \qquad \text{(eq. 3)}$$

where γ is the liquid fraction that has melted of the PCM. It varies from 0 to 1 depending on temperature variation compared to the melting temperatures.

A number of boundary conditions were implemented to account for the different configurations under study and for the different properties that each domain has. In the Single PCM configuration, thermophysical properties of the first PCM was applied to the whole PCM domain. In the M-PCMs - parallel arrangement, three PCMs surrounding each other fill three sections of the PCM domain while in the M-PCMs - in series configuration, the three PCMs sections are arranged next to each other. Properties of each PCM was applied to its section.

The working fluid flows in the inner pipe with constant inlet velocity of 0.9 m/s and temperature of 523.13 K and exits with fully developed flow characteristics. It is modeled as a transient laminar incompressible flow. As it flows, heat transfer occurs through the pipe wall and towards PCMs due to the temperature difference. PCMs are assumed to have an initial temperature of 423.13 k. Other assumptions are: No-slip boundary conditions, negligible viscous dissipation and no heat loss to the surroundings. All the thermophysical properties are constant except for the working fluid temperature dependent properties and the PCM's density

where Boussinesq approximation is used to model variations in the momentum equation resulting from density variations in fluids.

2.3 Computational Method

The governing equations were solved in the specified domain using transient numerical simulation with the aid of ANSYS FLUENT software that applies the finite volume method in discretized domain to solve the partial differential equations. To account for the PCMs melting, the "Solidification & Melting" model was used that considers the energy equation in the enthalpy form to account for the latent heat of melting. Simulation was accomplished by using the "Semi-Implicit Method for Pressure Linked Equations" "SIMPLE" algorithm and the pressure-based solver.

Model validation:

In order to test the validity of the developed model, a comparison with the study conducted by Fornarelli et al. [8] was done. That study investigated the use of phase change materials for high temperature applications using a shell and tube setup where PCM is contained in a cylindrical tank with heat transfer fluid flowing in an immersed steel tube from top to bottom. It was found in that study that natural convection enhances melting time considerably. This comparison considered the same exact geometry and boundary and initial conditions. Figure 3 shows comparison of the results obtained from the current model and that study at the same location. The temperature variation with time from both models are in reasonable agreement. The only disagreement between the models can be seen at the first half hour range. The reason for this is the fact that the temperature of the working fluid started at 423.13K and increased linearly until it reached 523.13K after 30 minutes in Fornarelli's study but this study considers the temperature of the working fluid to be 523.13 from start.

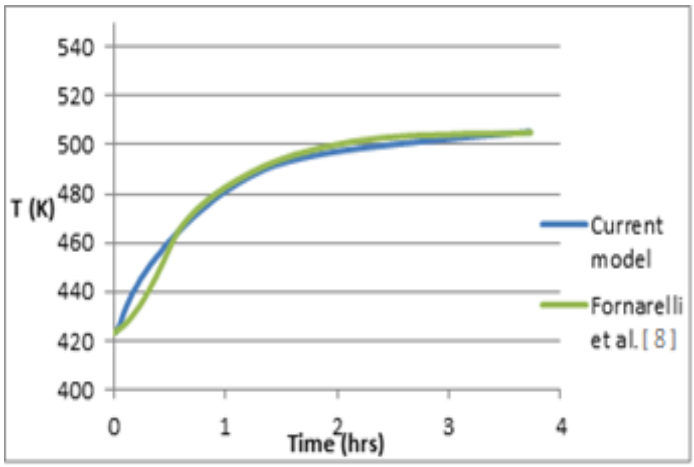

Fig. 3: Temperature variation with time at a specific location using current model and Fornarelli et al. [8]

3. Results and Discussion

In this section, contours of liquid fraction are presented to illustrate the melting process of the single PCM configuration compared to the m-PCMs configurations. Effects of the m-PCMs configuration on the heat transfer mechanisms are discussed.

3.1 Conduction heat transfer only (Case 1)

To investigate the performance of the different configurations based specifically on conduction heat transfer, natural convection is neglected. Since conduction heat transfer is not dependent on the direction of the gravity, this case represents both vertical and horizontal orientations. The indicated configurations of single, m-PCMs in series and in parallel were studied through numerical simulations. Single PCM configuration was tested first and was considered a base line on which comparisons with other configurations were made. Contours

representing melted PCMs versus time were plotted. Figure 4 shows liquid fraction contours for the single PCM configuration. It can be seen that the PCM is in solid state initially and as the working fluid starts flowing in the inner pipe, it starts heating up the walls of the pipe and consequently heats up the PCM until they reach their melting point where the melting process starts to take place. As time progresses, the melted layer grows by absorbing more heat from the working fluid. It can be seen how the low thermal conductivity affects this process negatively. The first layer adjacent to the wall melts relatively fast. However, the melting progress gets slower as the distance from the solid wall increases. One other reason for this is that heat transfer is directly proportional to temperature difference and as heat is transferred from the working fluid, there is a drop-in temperature difference. So, the second and third configurations come into the picture with m-PCMs with different melting temperatures (lower as the distance from inlet or from solid wall increases). The series configuration presented a promising start where the melting front started traveling faster than in the single PCM configuration. However, it slowed down toward the end with no significant overall enhancement. On the other hand, the parallel configuration presented significant enhancement and more consistent heat transfer performance. The melting front traveled with more uniform speed. When only conduction heat transfer considered, this configuration is found to reduce complete melting time by about 40% compared to the single PCM configuration.

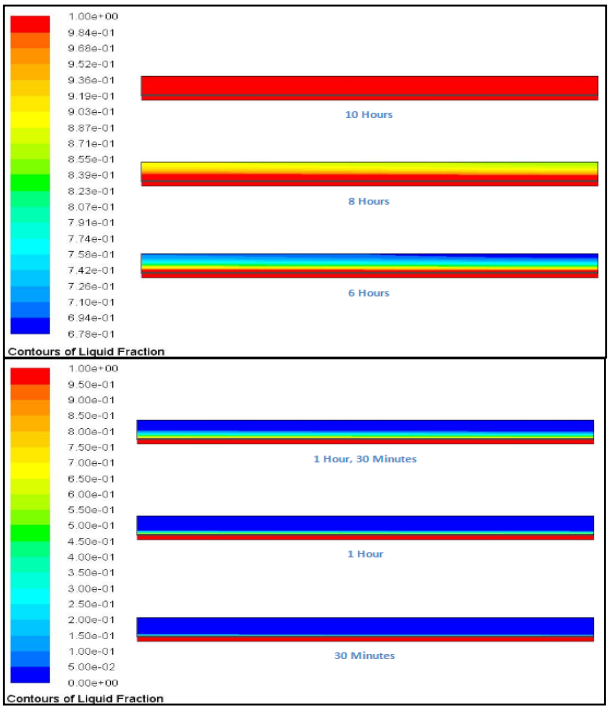

Fig. 4: Single PCM configuration – case 1

3.2 Conduction and natural convection in vertical orientation (Case 2)

This case considers both conduction and natural convection heat transfer mechanisms when the system is vertically oriented. Like case 1, contours of the liquid fraction were plotted. Examining the configurations, it was found that natural convection affects the heat transfer and the melted layer growth with clear reduction in melting time. Once a portion of the PCMs melts, it starts floating up. This circulation boosts the heat transfer. Figure 5 shows the series m-PCMS configuration in case 2 where huge enhancement is observed. This is about 47% reduction in complete melting time compared to the single PCM configuration in vertical orientation and about 60% reduction compared to case 1 (series configuration with conduction only). On the other hand, the parallel configuration in case 2 was found to perform slightly better than the single configuration but not as good as the series one with about 22% reduction in complete melting time compared to the single PCM configuration in vertical orientation. It also does not present significant enhancement over the parallel configuration in case 1 (less than 3% reduction in melting time). Moreover, comparing the series and parallel

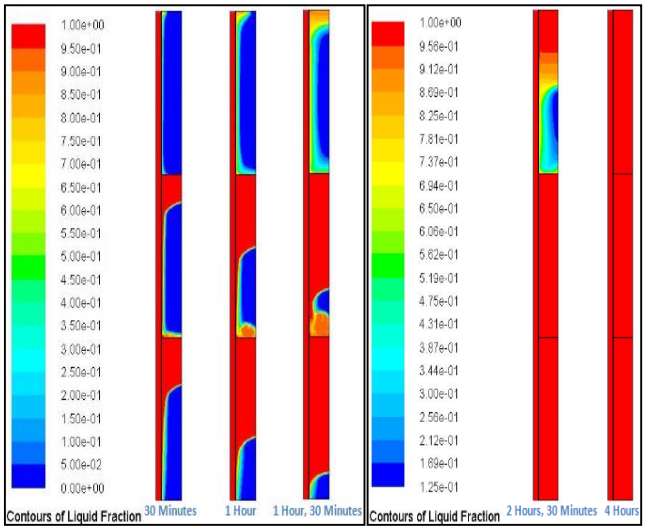

Fig. 5: M-PCMS in series configuration – case 2

configurations of both case 1 and case 2, they present opposite indications; in case 1, the parallel configuration was superior to the series configuration (40% vs 0% reduction in melting time compared to the single PCM1 configuration); while the opposite is observed in case 2.

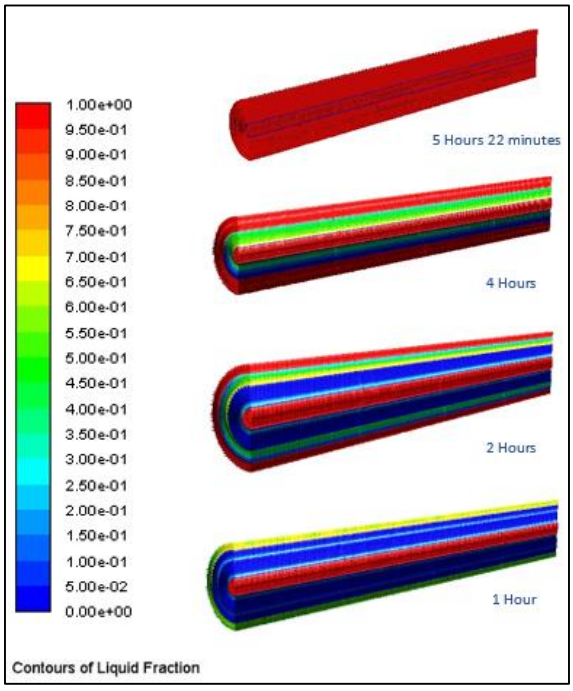

Fig. 6: M–PCMS parallel configuration – case 3

3.3 Conduction and natural convection in horizontal orientation (Case 3)

The axisymmetric assumption is invalid in this case due to gravitational force direction. The bottom part of the PCM containing tube have lower natural convection heat transfer rate compared to the top part as the pipe wall will suppress the buoyancy motion. This led to modeling this case in 3 dimensions. However, instead of modeling the complete concentric pipe, only half of it is considered due to symmetry., Figure 6 shows the liquid fraction contours for the parallel m-PCMs configuration in case 3. As was expected, the upper part of the PCM container has faster melting rate due to higher natural convection heat transfer rate compared to the lower part in all the three configurations. It was observed that both the series and the parallel configurations

enhanced the performance compared to the single PCM configuration (about 15.5% and 9.3% reduction in the melting time respectively). However, this enhancement is not as significant as the situation in case 2 (vertical orientation). On the other hand, the single PCM configuration in case 3 performs significantly better compared to both case 1 and case 2 (which shows about 41% and 21% reduction in melting time respectively).

4. Conclusion

This study investigated the performance of using multiple PCMs in different configurations and orientations. A discussion of the effects of conduction and natural convection heat transfer were studied. Results show that natural convection has a significant positive effect on the heat transfer characteristics of the systems. It was also found that the application of multiple PCMs generally enhances performance. However, they have different effects on the heat transfer mechanisms depending on configuration and orientation. Parallel configuration enhances conduction but suppresses natural convection while series does the opposite. It was also found that vertical orientation enhances natural convection more than the horizontal orientation for the multiple PCMs configurations. Energy storage with the series configuration in vertical orientation was found to be superior with 47% and 60% reduction in complete melting time respectively, compared to the single configuration in vertical orientation and the single and series configurations (horizontal and vertical) in the conduction only case.

Acknowledgements

This work used the Extreme Science and Engineering Discovery Environment (XSEDE), which is supported by National Science Foundation grant number ACI-1548562. Specifically, it used the Bridges system, which is supported by NSF award number ACI-1445606, at the Pittsburgh Supercomputing Center (PSC).

5. References

1. Dheep, G., Sreekumar, A., 2014. Influence of nanomaterials on properties of latent heat solar thermal energy storage materials – A review. Energy Conversion and Management. 83, 133-147.
2. Li, T., Lee, J., Wang, R., Kang, Y., 2014. Heat transfer characteristics of phase change nanocomposite materials for thermal energy storage application. International Journal of Heat and Mass Transfer. 75.
3. Sahan, N., Paksoy, H., 2014. Thermal enhancement of paraffin as a phase change material with nanomagnetite. Solar Energy Materials & Solar Cells. 126.
4. Zabalegui, A., Lokapur, D., Lee, H., 2014. Nanofluid PCMs for thermal energy storage: Latenet heat reduction mechanisms and a numerical study of effective thermal storage performance. International Journal of Heat and Mass Transfer. 78, 1145-1154.
5. Peiro, G., Gasia, J., Miro, L., Cabeza., 2015. Experimental evaluation at pilot plant scale of multiple PCMs (cascaded) vs. single PCM configuration for thermal energy storage. Renewable Energy. 83, 729-736.
6. Aldoss, T., Rhman, M., 2014. Comparison between the single-PCM and multi-PCM thermal energy storage design. Energy Conversion and Management. 83, 79-87.
7. Wang, P., Wang, X., Huang, Y., Li, C., Peng, Z., Ding, Y., 2015. Thermal energy charging behaviour of a heat exchange device with a zigzag plate configuration containing multi-phase-change-materials (m-PCMs). Applied Energy. 142, 328-336.
8. Fornarelli, F., Camporeale, S. M., Fortunato, B., Torresi, M., Oresta, P., Magliocchetti, L., Miliozzi, A., Santo, G., 2016. CFD analysis of melting process in a shell-and-tube latent heat storage for concentrated solar power plants. Applied Energy. 164, 711-722.

Conference
Proceedings

ASES National Solar Conference 2019
Minneapolis, MN, USA, 05 – 09 August 2019

Evaluation of an Integrated Pipe Water Cooling Strategy to Improve BIPV Structure Performance

Isaac Gendler[1,2] Mara Leandro[1], Ramina Albazi[1] , Rodrigo Henriquez[1], Josh Sanghvi[1], Reshma Singh[2] ,Gayathri Aaditya Eranki[2], Sohail H. Zaidi[1]

[1] San Jose State University, San Jose (U.S.A)

[2] Lawrence Berkeley National Laboratory, Berkeley (U.S.A)

1. Abstract

When the temperatures of photovoltaics break a threshold of 25 degrees celsius, they begin to lose efficiency. This work describes the basis of a water cooling mechanism which may be used to cool down roof mounted photovoltaics. After a thorough literature review, it was decided that running water through aluminum pipes attached to the back of a solar panel would be the most effective method. To study the effectiveness of such a system, a prototype was fabricated two panels were brought out to the top of a solar deck in an engineering university building and laid out in parallel. One panel had the cooling system attached to its back and the other one had no attachments to serve as a control panel. Experimentation was performed by taking temperature measurements for one hour before activating the hydraulics for 30 minutes. It was found that a significant reduction of temperature occurred on the water-cooled panel.

Keywords: *Solar power, buildings, thermodynamics, cooling,*

2. Introduction

With the advent of global climate change, human civilization will have to plan for the future and overhaul existing critical infrastructure with sustainability and resilience in mind. A key element to this will be the deep decarbonization of the energy sector. One of the most promising technologies is the deployment of rooftop solar panels, known in many technical circles as Building-Integrated Photovoltaics. However, the performance of these systems are not immune to ambient environmental conditions. In particular, it has been found that with every degree centigrade above 25 C(Pillai et. al) the electricity efficiency decreases by upwards of 0.5%. This will be especially harmful to communities who inhabit hotter climates and the global south, where the intensity of the sunlight is much greater.

These issues can be greatly mitigated through the application of cooling techniques to solar panels. By enabling solar energy generation to operate at a lower temperature, efficiency can be greatly improved. This will

doi:10.18086/solar.2019.01.01 Available at http://proceedings.ises.org

assist areas with warm ambient climates in implementing distributed energy resources and transition to a carbon free economy.

3. **Literature Review**

Before deciding on a specific technology, a literature review was undertaken.

3.1 Liquid Immersion

Liquid immersion consist of solar panels being immersed in a thin layer of a liquid to maintain lower temperatures. Liquids such as non-polar silicon oil, polar ethanol, glycerin, non-polar benzene, inorganic distilled water, and tap water have been tested, with some being more effective than others.
The performance of bare cells and a solar panel were examined with different liquids immersed at different depths by Abrahamyan et al (2001). It was determined that bare solar cells immersed in non-polar silicon oil performed the best. The cells increased their efficiency by 4.07% while immersed at 9 mm, compared to a 3.78% and 3.49% efficiency at 3 and 6 mm, respectively. At wide temperature ranges, silicon oil has a high chemical stability, good weather resistance, and has low surface tension. These physical and chemical performances make silicon a good candidate for high temperature and long service applications. Although, silicon-oil might be an alternative to keeping solar panels cool, the cost of this liquid is not economical. One of the goals of this project is to provide a cost-effective cooling system for solar panels, therefore this method would not meet this goal.

Rosa-Clot et al. (2010) compared the performance of three photovoltaic panels, two of which were immersed at 4 cm and 40 cm in water and one that was at ambient temperature. According to Rosa-Clot et al. there are two main effects that increase the efficiency of a commercial panel placed in water, the first is the reduction of light reflection and secondly, the absence of thermal drift. Thermal drift refers to the change in the normal operational behavior of a device due to changes in ambient temperature. It was concluded that the efficiency increased or reduced depending on the depth the photovoltaic panel was immersed in, as shown below in Fig. 1.

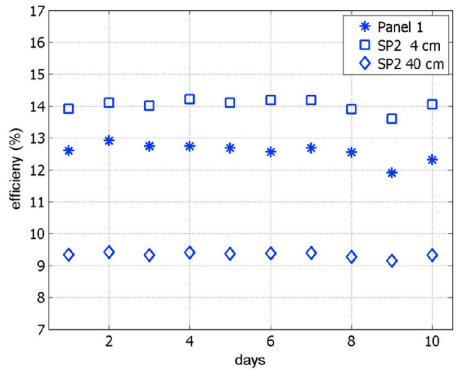

Figure 1: Comparison of the three photovoltaic panels in different ambients all tested for a period of 10 days (Rosa-Clot et al.(2010))

3.2 Phase-Changing Materials

Phase-Changing Materials (PCMs) are materials which are at the interphase point in ambient temperatures. This allows them to absorb large amounts of latent heat before changing their temperature, making them extremely effective as passive heat skins.
These properties have made PCMs a captivating topic for numerous researchers. A one-dimensional heat transfer model usable for simulation was developed for combined PV-PCM systems (Kibira 2016). This was further expanded upon in later work with the creation of a two-dimensional heat transfer model for the system but also

empirically evaluated the effectiveness of a PCM system with different fin configurations (Huang et. al 2018). Adding fins were also shown to be beneficial of the PV system (Khanna et. al (2018)) (Ma. et.al (2015)).
Field testing for the economic effectiveness of PV-PCMs in Ireland and Pakistan was carried out by Hasan et. all which revealed that PV-PCM systems were economically in hot climates similar to the latter but ineffective in the former's (Hasan et. al 2014). Since San Jose's mild temperature norms puts in in the middle of the aforementioned areas, it would very likely be at the breakeven cost point. A list and testing of five possible PV-PCM materials was also compiled (Hasan et. al. 2010). Ultimately, the high initial cost of PCMs outweighed their utility and made them unsuitable for our study. After obtaining the cost of materials and possible efficiency in a mild climate, it did not appear effective for utilization.

3.3 Water Trickling

Another promising cooling strategy is to utilize water trickling down the front surface of the panel. This will not only cool down the panel itself by also clean it up ony residue, thereby increasing its efficiency. Work by Schiro et. al. (2017) found that a uniform spreading of water would achieve the greatest results.

4. **Design**

4.1 Theory

The cooling system design selected worked as follows. Water is passed through a series of horizontal square aluminum pipes attached to the back of a solar panel. The flowing water absorbs heat from the panel, thereby cooling it. The heated water at the end is either discarded or recycled depending on the setup of the system. Since the literature stated that the optimal temperature for solar panels was 25 degrees celsius, that became the target temperature for the system.

4.2 Setup

The systems design can be seen in Fig. 2**.** The cooling system uses PVC as the inlet for water flow. Clear acrylic tubing would then connect the PVC to square aluminum pipes. These pipes are attached to the back of the PV panel using thermal paste. Water exits the aluminum pipes, through acrylic tubing and out through PVC.

The component descriptions are listed below.

Component	Description
Rectangular Aluminum Pipe	8 - 1”x1”x48”
PVC Clear Vinyl Tube	7/8 in. O.D. x 5/8 in. I.D. x 10 ft.
PVC Schedule 40 Plain-End Pipe	1 in. x 10 ft.
Tube Heat Sink Compound	3 oz.
Heavy Duty Duct Tape	1-7/8 in. x 13.2 yds.

Tab. 1 - System components

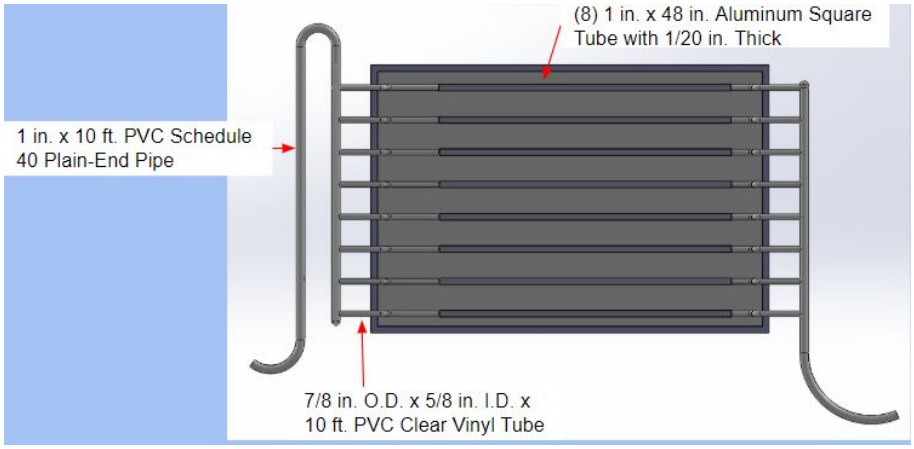

Figure 2: Design of Cooling System

4.3 *Physical Implementation*

Implementation of system designed is shown in Fig. 3.

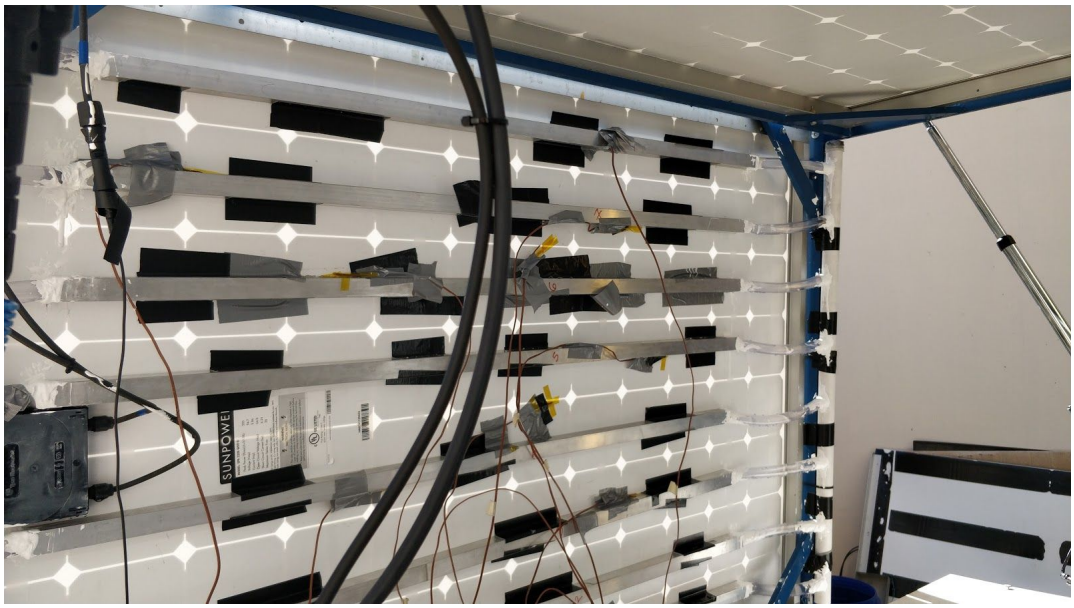

Fig 3 - Implemented system

5. Experimentation

5.1 Setup

For the experiment, a triple Sunpower SPR-320E-WHT-D 320W Solar PV panel rack oriented south-west were used for the base model. The front panel was laid out horizontally such that it was parallel to the middle panel. The front panel had the cooling system attached while the middle was used as a control panel. This was done so each panel would receive equal irradiation and therefore have identical temperature signatures before any cooling was applied, allowing for a more objective analysis of the system performance. The solar panel rack came with a host of other solar PV system components such as charge controllers and a battery. This setup can be seen in Fig. 4, with the cooled panel overlaid in blue and the base panel in red.

Figure 4 - The Solar Rack Setup

5.2 Tools

14 T-type thermocouples with an accuracy of +- 0.1 C were used to carry out temperature measurements. These were spread across the back of the PV panel parallel to one another to obtain surface temperature readings. The back of the panel was chosen since it would be the closest to the proposed piping system. The position of each thermocouple can be seen in Fig. 5. These were connected to an Agilent 34970a DAQ System with a sampling rate of one reading per minute.

Three 3 LI-COR - LI-200SA Pyranometers were used to measure the incident irradiation on the solar panels. These were placed on the top of the front-facing solar panel in the rack (two on each end and in the middle) and connected to a three-channel Li-Cor 1500 Logger.

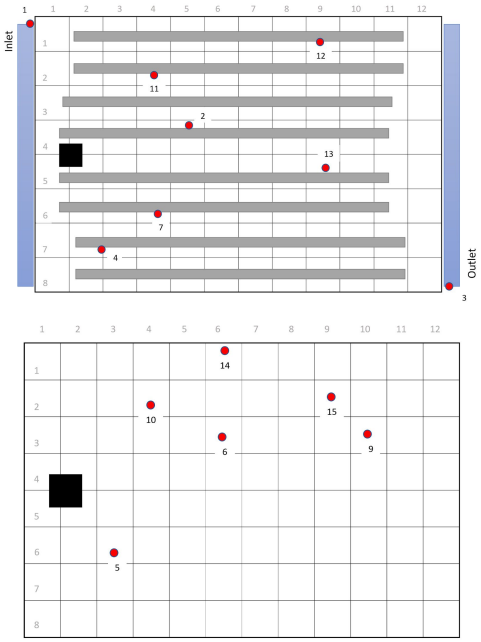

Figure 5: Map of backside thermocouples. The numbers correspond to the thermocouple on the DAQ system

5.3 Procedure

The testing procedure was straightforward. At around 1:30 pm on April 24th 2019, the thermocouple loggers were activated. These would take data at a rate of one sample per minute for an hour before the water pump was switched on. Data would be taken for another 30 minutes. From this, It can be seen not only the effect of water on panel temperatures but also how it compares to a panel which receives no applied cooling

5.4 Results

The results from experimentation can be seen in Fig 6. Once water cooling was activated, the solar panel with the system attached was able to experience a drastic temperature drop along with the inlet and outlet water temperature. The minimum average temperature at the back panel with cooling after activation was 36.9 degrees C, compared to 48.9 degrees C for the control panel, even though it was at a higher temperature before activation. The minimum average temperature was 32.4 degrees C, which is 7.4 degrees higher than the desired temperature of 25 degrees C. It is important to note that the ambient temperature at the day of experiment was 32.2 C (Weather San Jose CA 95112 April 24th 2019. (2019, April 24)), making it extremely difficult to achieve the desired temperature of 25 degrees C. Surprisingly outlet water temperature was only slightly higher than the inlet temperature. This indicates that due to higher thermal conductivity of aluminum the heat was dissipated from water through aluminum structure.

As seen in Fig. 7, the irradiance over time was fairly constant. As there was no significant change in irradiation, the results should not have been affected too drastically.

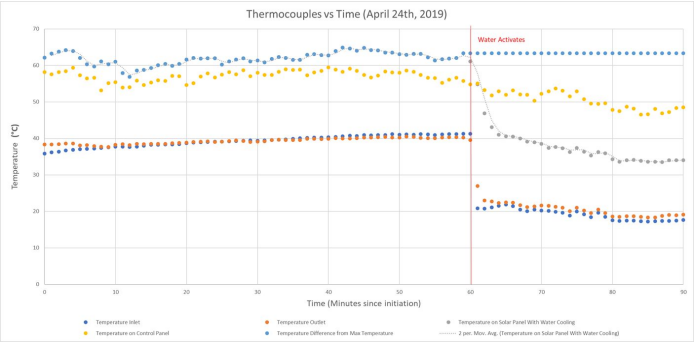

Figure 6: Thermal data over the period of the experiment

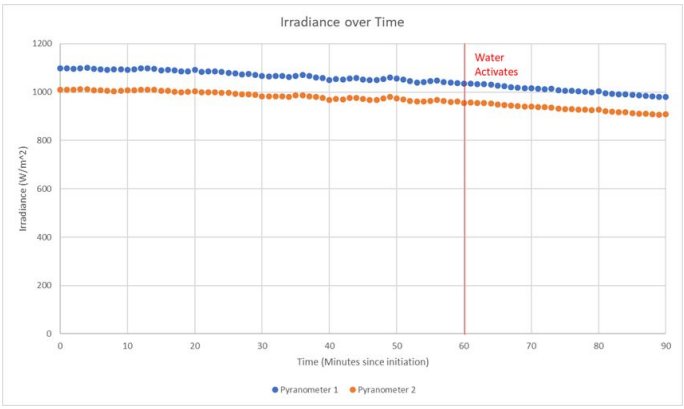

Figure 7: Irradiance data over the period of the experiment

6. **Thermal Analysis**

Theoretical calculations were needed to compare both the experimental and simulation results. The point of interest was the panel's back surface temperature to compare to readings given by the thermocouples. To obtain this temperature a thermal resistance network needed to be analyzed. Thermal resistance of the solar panel, or any other medium, depends on its geometry and thermal properties. In this case, the thermal resistance of the panel was assumed to be in series, with the map seen in Fig. 8. Therefore, the equivalent thermal resistance is determined by adding the individual resistances, **Eq (1)**. Basic knowledge about the following parameters must be known: ambient temperature, wind velocity, and irradiation at the time of the experiment for all boundary conditions. Other parameters needed to be calculated for the set up were the convection coefficients and the total heat resistance of the panel without and with the cooling system.

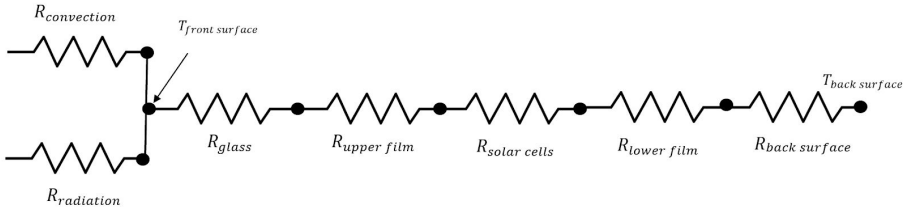

Figure 8 - Thermal Resistance Network

$$R_{total} = R_{conv\ and\ rad} + R_{glass} + R_{upper\ film} + R_{solar\ cells} + R_{lower\ film} + R_{back\ surface}\ [\frac{℃}{W}] \quad \textbf{(1)}$$

Where resistance R_{conv} , R_{cond}, R_{rad} for each material are the following.

$$R_{conv} = \frac{1}{hA_s}\ [\frac{℃}{W}] \quad \textbf{(2)}$$

$$R_{cond} = \frac{L}{kA_s}\ [\frac{℃}{W}] \quad \textbf{(3)}$$

$$R_{cond} = \frac{1}{h_{rad}A_s}\ [\frac{℃}{W}] \quad \textbf{(4)}$$

As seen from the thermal resistance network, most solar panels consist of five thermal conductive materials which are the anti-reflective glass, the upper encapsulating film (EVA), solar cells, the lower encapsulating film (EVA), and the tedlar laminated film (back surface). Thermal conductivity and thickness of each material, and surface area of the solar panel, were needed to determine individual thermal resistances, and eventually the equivalent resistance. Temperature of the back surface can be determined if the heat transfer, Qdot, and the ambient temperature are known, **Eq. (5)**.

$$\dot{Q} = \frac{T_{back\ surface} - T_{ambient}}{R_{total}} \quad \textbf{(5)}$$

From the equation above it is notable that the rate of heat transfer between the two surfaces is equal to their temperature difference divided by the total thermal resistance of the solar panel.
Using Equations 1-5, a back surface temperature of 58.2 ℃ was determined. Comparing this result to the highest temperature read by the thermocouples, 59 ℃, there is a percent error of about 1.4.

7. Conclusion and Future Work

7.1 Conclusion

A proposed water cooling system for building-integrated photovoltaics was developed and manufactured. Through experimentation, we were able to validate that it was able to provide effective cooling for a solar panel. The minimum average temperature at the back panel with cooling after activation was 36.9 degrees C, compared to 48.9 degrees C for the control panel. The minimum average temperature was 32.4 degrees C, which is 7.4 degrees higher than the desired temperature of 25 degrees C.

It is important to note that the ambient temperature at the day of experiment was 32.2 C, making it extremely difficult to achieve the desired temperature of 25 degrees C. Surprisingly, outlet water temperature was only slightly higher than the inlet temperature. This indicates that due to higher thermal conductivity of aluminum the heat was dissipated from water through aluminum structure.

7.2 Future Work

Future work on this project should concentrate on shifting the system to a passive cooling solution, where no active energy input needs to be used. This can be accomplished through heat pipes and natural heat sinks. In addition, one of the chief priorities for the system redesign should be to make it such that it can be commercially implementable into a building. This will enable the technology to be dispersed throughout the world and assist in achieving deep decarbonization. Regarding the CFD simulation, future work on this regard would consist on using the ANSYS thermal calculator to obtain more accurate irradiation data rather than data obtained from the pyrometer.

8. **References**

Abrahamyan, Serago, Aroutiounian, Anisimova, Stafeev, Karamian, . . . Mouradyan. (2002). The efficiency of solar cells immersed in liquid dielectrics. Solar Energy Materials and Solar Cells, 73(4), 367-375. Retrieved from https://doi.org/10.1016/S0927-0248(01)00220-3

Hasan, A., Josephine-McCormack, S., Huang, M., & Norton, B. (2014). Energy and cost saving of a photovoltaic-phase change materials (PV-PCM) system through temperature regulation and performance enhancement of photovoltaics (7th ed.) Energies. doi:- 10.3390/en7031318

Hasan, A., McCormack, S. J., Huang, M. J., & Norton, B. (2010). Evaluation of phase change materials for thermal regulation enhancement of building integrated photovoltaics doi:https://doi.org/10.1016/j.solener.2010.06.010

Khanna, S., Reddy, K. S., & Mallick, T. K. (2018). Optimization of finned solar photovoltaic phase change material (finned pv pcm) system doi:https://doi.org/10.1016/j.ijthermalsci.2018.04.033

Kibria, M. A., Saidur, R., Al-Sulaiman, F. A., & Aziz, M. M. A. (2016). Development of a thermal model for a hybrid photovoltaic module and phase change materials storage integrated in buildings doi:https://doi.org/10.1016/j.solener.2015.11.027

Lim, J.-H., Lee, Y.-S., & Seong, Y.-B. (2017). Diurnal Thermal Behavior of Photovoltaic Panel with Phase Change Materials under Different Weather Conditions. Energies, 10(12), 1983. MDPI AG. Retrieved from http://dx.doi.org/10.3390/en10121983

Ma, T., Yang, H., Zhang, Y., Lu, L., & Wang, X. (2015). Using phase change materials in photovoltaic systems for thermal regulation and electrical efficiency improvement: A review and outlook doi:https://doi.org/10.1016/j.rser.2014.12.003

Rosa-Clot, M., Rosa-Clot, P., Tina, G.M., & Scandura, P.F. (2010). Submerged photovoltaic solar panel: SP2. Renewable Energy, 35(8), 1862-1865. Retrieved from https://doi.org/10.1016/j.renene.2009.10.023

Schiro, F., Benato, A., Stoppato, A., & Destro, N. (2017). Improving photovoltaics efficiency by water cooling: modelling and experimental approach. Energy, 137, 798-810.

Weather San Jose CA 95112 April 24th 2019. (2019, April 24). Retrieved May 11, 2019, from https://www.wunderground.com/history/daily/us/ca/san-jose/KSJC/date/2019-4-24

S

Z